International Journal of Heat and Mass Transfer 164 (2021) 120533

Contents lists available at ScienceDirect

International Journal of Heat and Mass Transfer

journal homepage: www.elsevier.com/locate/hmt

Effects and mechanism of filler surface coating strategy on thermal conductivity of composites: A case study on epoxy/SiO_2-coated BN composites

Yunmin Liang, Biwei Liu, Bo Zhang, Zhichun Liu*, Wei Liu

School of Energy and Power Engineering, Huazhong University of Science and Technology, Wuhan, 430074, China

ARTICLE INFO

Article history:
Received 15 May 2020
Revised 2 September 2020
Accepted 24 September 2020

Keywords:
Polymer-matrix composites
Thermal conductivity
Nanolayer coating strategy
Interfacial thermal resistance
Effective filler volume fraction

ABSTRACT

In order to make a systematic understanding of the effects and mechanism of the filler surface coating strategy on the thermal conductivity of composites, the silica coated BN was synthesized via Stöber sol-gel method and then incorporated into epoxy. The thermal conductivities of epoxy/BN@SiO_2 composites were investigated experimentally, and it was found that increasing the coating thickness or filler content would decrease the enhanced effect of the strategy on thermal conduction. Fitting the thermal conductivities of composites with the EMA model indicates that the interfacial thermal resistance in the formed BN@SiO_2 thermal conduction networks will increase with the increase of filler content, and then deteriorates the thermal conduction enhancement factor. Thus, the concept of the effective filler volume fraction was introduced in the strategy for the first time. Reducing the coating thickness will expand the effective filler volume fraction, but the upper limit of the effective filler volume fraction will not exceed the maximum random packing volume fraction of the fillers. The mechanism research provides an efficient guideline for further studying core-shell particles to improve the thermal conductivity of composites.

© 2020 Elsevier Ltd. All rights reserved.

1. Introduction

Polymer-matrix composites possess wide applications as thermal management materials in electronic package [1–3]. The intrinsic thermal conductivity of polymer is extremely low and improving the thermal conductivity of polymer materials by the incorporation of fillers with high thermal conductivity is a promising method [4–6]. In past experimental researches, the category, shape, and size of the fillers were commonly taken into account to enhance the thermal conductivity of polymeric composites [7–10]. In fact, the bad miscibility and poor affinity between the fillers and polymer matrix significantly damage the thermal conductivity of composites [11–14]. In order to improve the chemical and physical structure of the filler surface, which is a key parameter in determining the dispersion and interfacial interaction, coating the filler surface with a nanolayer has been proved as an effective strategy [15–21]. Diverse surface coating routes such as the sol-gel method, direct impregnation technique, and dopamine chemistry have been developed [22–25]. Shen et al. [15] prepared PVA/BN composite films and the results demonstrate that polydopamine coated h-BN fillers are well dispersed in the PVA matrix and achieve a stronger thermal conductivity enhancement than pristine h-BN. Chen et al. [17] synthesized silica-coated silver nanowires and incorporated them into an epoxy matrix. At the same loading of nanowires, the epoxy/AgNWs@SiO_2 composites exhibit higher thermal conductivity than that of the epoxy/AgNWs composites. Yan et al. [23] prepared polyimide nanocomposites with BN-coated multiwall carbon nanotubes. When filler loading was 3.0wt%, the thermal conductivity of the PI/WMCNT@BN composites was almost twice of that of the PI/WMCNT composites. However, the effects of using the strategy are not always as expected. In some cases, otherwise, the nanolayer coated on the filler surface could deteriorate the thermal conduction in the composites. The TiO_2 coated AgNW was synthesized in the work of Jiang et al. [25]. At the whole filler content ranges, the AgNW@TiO_2 has negative effects on the thermal conductivity of composites. The negative effects of the nanolayer on the thermal conductivity were also observed in alumina-coated graphene and silica-coated graphite polymer composites [26,27]. Some experimental researches have been conducted to investigate which factor plays a role in the strategy and how they affect the thermal conduction in the composites [28,29]. But a comprehensive and accurate understanding is still not formed and more efforts remain to be made to systematically investigate this issue.

* Corresponding author: 1037 Luoyu Road, Hongshan District, Wuhan 430074, China.

E-mail address: zcliu@hust.edu.cn (Z. Liu).

https://doi.org/10.1016/j.ijheatmasstransfer.2020.120533
0017-9310/© 2020 Elsevier Ltd. All rights reserved.

Herein, the representative BN/epoxy system was selected and the classic Stöber sol-gel method was used in the strategy to coat a compact silica network on the surface of BN to improve the surface chemical inertness. Through the full characterization of the BN@SiO_2 and its epoxy-based composites, the effects and mechanism of coating the filler surface with a nanolayer on the thermal conductivity of composites were systematically analyzed and clearly presented.

2. Experimental work

2.1. Materials

The BN powder (diameter of 3~5 μm) was purchased from Qinghe Xintie Metal Material Co., Ltd. (China). Ethanol, acetone, ammonium hydroxide (NH_4OH), tetraethyl orthosilicate (TEOS), deionized water and the curing agent 4,4÷diaminodiphenylsulfone (DDS) were purchased from Sinopharm Chemical Reagent Co., Ltd. (SCRC, China). In addition, commercial epoxy resin diglycidyl ether of bisphenol-A (E-51) was purchased from Baling Petrochemical Co., Ltd. (China).

2.2. Synthesis of SiO_2-coated BN

The successful synthesis of silica nanolayer coated BN was using the Stöber sol-gel method [22,30]. A typical synthesis process was demonstrated as follows. 3 g BN powder was ultrasonically dispersed in the mixture of 200 mL anhydrous ethanol, 30 mL NH_4OH, and 40 mL deionized water and then vigorously magnetic stirred for 30 min to obtain a homogeneous suspension. Next, 10 mL of TEOS was added slowly and the mixture was continuously stirred for 6 h at room temperature. After the reaction, the product was vacuum-filtered through a Nylon membrane and washed with ethanol and deionized water sequentially. The process was repeated several times to remove the free SiO_2 particles and then vacuum drying to obtain the SiO_2-coated BN white powder. The thickness adjustment of silica nanolayer was mainly achieved by changing the usage amount of TEOS. Herein, to obtain a thinner silica nanolayer, 2 mL of TEOS was added in the synthesis process as mentioned above. In contrast, 20 mL of TEOS was added in the same synthesis process to increase the silica nanolayer and subsequent purification processes were carried out as above.

2.3. Preparation of epoxy/BN@SiO_2 composites

The BN@SiO_2 powder was mixed with the desired amount of epoxy resin and DDS (34wt% relative to epoxy) in acetone. The blend was ultra-sonicated for 2 h at room temperature and then vigorously stirred at 60 °C until the weight was constant to obtain the BN@SiO_2 evenly dispersed epoxy slurry. The mixture was degassed at 80 °C to remove any trapped air bubbles and residual acetone. Then the mixture was cast in steel molds and cured at 130 °C for 2 h, 190 °C for 3 h, followed by post-cure at 210 °C for 1 h. After the cure program, the disk-like epoxy/BN@SiO_2 composite was obtained. Herein, the content of BN@SiO_2 in the composite was fixed at 10, 20 and 30 vol.%, respectively. For comparison, the pure epoxy resin and epoxy/BN composites with the same filler content were prepared following the same procedure described above.

2.4. Characterization

Fourier transform infrared (FT-IR) spectra were obtained using a Bruker Vertex 70 FTIR spectrophotometer with the standard KBr pellets method to study the variation on the surface structures of the BN powder. Transmission electron microscopy (TEM, Tecnai G220, Netherlands) was used to confirm the core-shell nanostructures of SiO_2-coated BN. The morphologies and dispersions of BN and BN@SiO_2 in the composites fracture surfaces were observed using scanning electron microscopy (SEM, Nova NanoSEM450, Netherlands). X-ray photoelectron spectroscopy (XPS) was conducted on an ESCALAB 250Xi spectrometer (Thermo Fisher Scientific Inc., USA) to measure the element components on the surface of BN and BN@SiO_2. The crystal structure of the BN@SiO_2 was analyzed using an X-ray diffractometer (XRD, X'Pert3 Powder, Netherlands) with Cu Kα radiation. Thermal conductivity was measured by XIATECH TC3000 thermal conductivity analyzer (Xi'an Xiatech Electronics Co. Ltd., China) by using the transient hot-wire method at room temperature. To reduce the contact thermal resistance between the probe and sample, the surfaces of the cured composites were well polished. The dynamic mechanical analyzer (DMA) of EP composite was conducted on a Diamond DMA (Perkin-Elmer Inc., USA). The samples with the dimension of 10 × 20 × 2 mm were tested in a tension mode at a constant frequency of 1 Hz and heated from 30 °C to 250 °C at a rate of 3 °C/min (DMA analysis of the composites is presented in the supporting information).

3. Results and discussion

3.1. Characterization of BN@SiO_2 and its epoxy-based composites

The changes in surface element components of pristine BN and BN@SiO_2 were examined by XPS analysis and the results are shown in Fig. 1. The peaks at 104, 154, 190, 398 and 533 eV can be assigned to Si 2p, Si 2 s, B 1 s, N 1 s, and O 1 s, respectively. Compared with pristine BN, the presence of Si 2p and Si 2 s and the significantly increased peak intensity of O 1 s are observed in the XPS spectrum of BN@SiO_2, which can be attributed to the compact coating of silica network on the surface of BN. The chemical groups on the surface of pristine BN and BN@SiO_2 were analyzed by FT-IR, and the results are shown in Fig. 2. In the spectrum of BN@SiO_2, the broad absorption band centered at 3416 cm^{-1} is assigned to the hydroxyl group. The intense Si–O–Si bond stretching vibrations appear at 1084 cm^{-1} revealing the existence of a dense silica network and the Si–O in-plane stretching vibrations of the silanol groups Si–OH appear at 951 cm^{-1}. Furthermore, the peak appears at 459 cm^{-1} is corresponding to the bending vibrations of the O-Si-O bond [31]. Due to the chemical inertness of BN, only B-N stretching peak at 1374 cm^{-1} and the B-N-B bend-

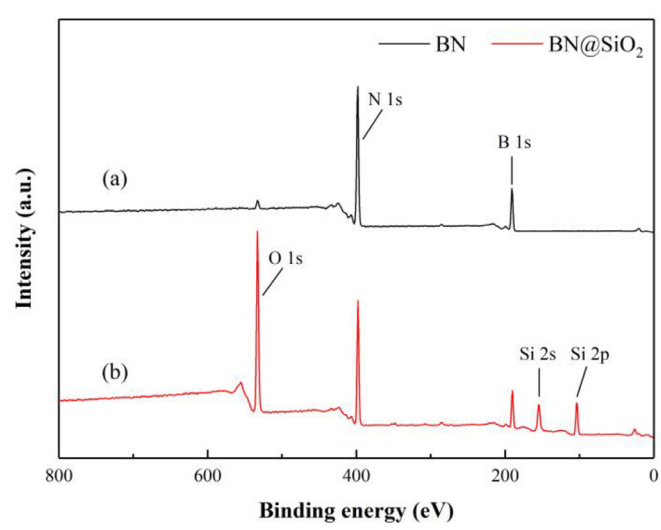

Fig. 1. XPS spectra of (a) pristine BN and (b) BN@SiO_2.

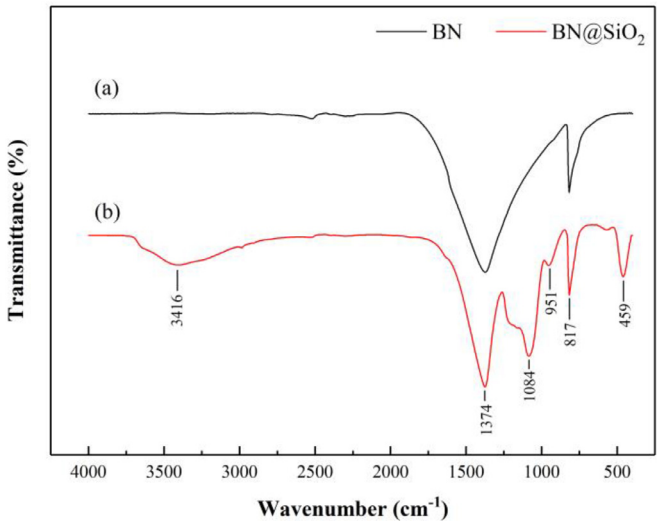

Fig. 2. FT-IR spectra of (a) pristine BN and (b) BN@SiO_2.

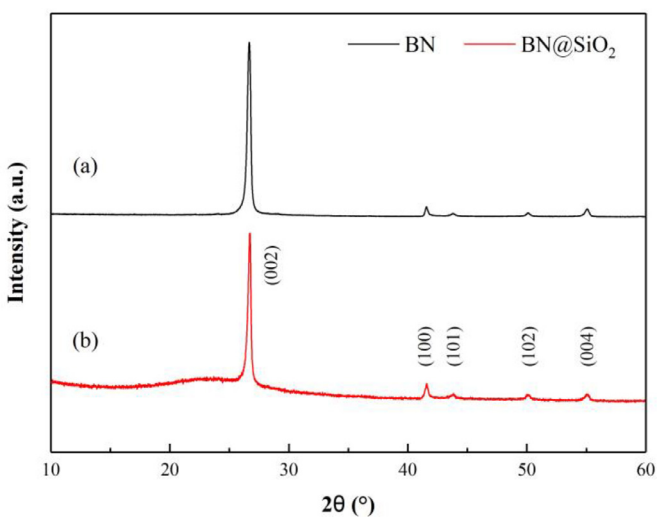

Fig. 3. XRD patterns of (a) pristine BN and (b) BN@SiO_2.

ing peak at 817 cm^{-1} are observed in the spectrum of pristine BN [32]. The XRD patterns of pristine BN and BN@SiO_2 are shown in Fig. 3. The diffraction peaks in the XRD pattern of BN at 26.7, 41.6, 43.8, 50.1 and 55.1° can be indexed to (002), (100), (101), (102) and (004) planes of hexagonal phase [33]. Compared with pristine BN, a weak and wide diffraction peak appeared at 22° in the XRD pattern of BN@SiO_2, which can be assigned to an amorphous SiO_2 nanolayer [34]. The morphologies of pristine BN and silica-coated BN were observed by SEM and TEM and the results are displayed in Fig. 4. As shown in Fig. 4(A) and (B), the SiO_2 particles were clustered and fused to form an amorphous silica network on the surface of BN during sol-gel processing [30], therefore, the surface of silica-coated BN is obviously coarser than that of the pristine BN. And the mono-dispersed SiO_2 spheres are not observed after the purification process. The core-shell nanostructures of BN@SiO_2 are clearly distinguished by TEM analysis and the average coating thickness is near 15 nm (Fig. 4D), 50 nm (Fig. 4E) and 70 nm (Fig. 4F), respectively. Based on the above discussion, BN@SiO_2 powder was successfully synthesized and the thickness of the silica nanolayer was successfully adjusted by changing the usage amount of TEOS.

The fracture surface morphology and dispersion of BN and BN@SiO_2 in the epoxy composites are shown in Fig. 5. As shown in Fig. 5A and B, there was no obvious morphology difference between the two composites at low filler content (10 vol.%). When the filler content increased to 20 and 30 vol.%, some agglomerates of BN were found in Fig. 5C and E and the dispersion of BN in the epoxy matrix was rapidly deteriorated, which may be due to the chemical inertness of the BN leading to a poor interfacial interaction in the polymer matrix [35]. Compared with the pristine BN, the silica coating layers of the BN@SiO_2 make the BN surfaces full of hydroxyl groups and improve the wettability between the BN and polymer matrix [17,19]. In addition, the reactions between the epoxy groups and silanol groups on the surface of BN@SiO_2 enhance the interfacial interaction in the composites [36]. Hence, as shown in Fig. 5D and F, the dispersion of BN@SiO_2 was more homogeneous than that of the pristine BN in the matrix even at a large filler content.

3.2. Effects and mechanism of the filler surface coating strategy on the thermal conductivity of composites

It's not hard to realize that the factors which can be intervened or controlled are not much when coating nanolayer on the filler surface. Although many filler surface coating routes can be selected, the material of nanolayer is unchangeable in a definite nanolayer coating strategy. Herein, because of abundant hydroxyl groups on the silica nanolayer, the classic Stöber sol-gel method was used to improve the chemical inertness of BN. More attention was paid to investigate the effects and mechanism of both coating thickness and filler content on the thermal conductivity of composites.

The powder of BN@SiO_2 with different coating thickness was incorporated into the epoxy at 10, 20 and 30 vol.% loading. For comparison, the pure epoxy and epoxy/BN composites at the same filler content were well prepared, too. The thermal conductivities of those samples are shown in Fig. 6. As shown in Fig. 6, the thermal conductivity of epoxy matrix is undesirable. With the incorporation of BN and BN@SiO_2, the thermal conductivities of composites were extremely enhanced as the filler content increased. Indeed, the effects of the filler surface coating strategy on the thermal conductivity of composites are complicated. When filler content was 20 vol.%, the epoxy composites incorporated with BN@SiO_2(15 nm) shown a higher thermal conductivity than that of the composites incorporated with the pristine BN. However, with increasing the thickness of silica nanolayer to 70 nm, the effects of the strategy have changed dramatically and the silica nanolayer deteriorated the thermal conduction in the composites. Although, the nanolayer coating strategy does enrich the chemical groups on the filler surface and enhance the interfacial interaction between the filler and polymer matrix. The thermal conductivity of the coating nanolayer is generally lower than the filler in the strategy. With increasing the thickness of coating nanolayer, the heat transfer is restrained significantly in the nanolayer, resulting in a huge interfacial thermal resistance between the filler and polymer matrix. Besides, the phonon scattering at the increased interfaces between the fillers and polymer matrix also deteriorates the thermal conduction in the composites. Therefore, at one fixed filler content, the thermal conductivity of composites is decreased by increasing the nanolayer coating thickness in the strategy. And the thermal conduction behavior is consistent with the reported work which investigates the thermal conductivity of composites filled with core-shell particles [37]. Especially, when a thick nanolayer is coated on the filler surface, the thermal conduction enhancement of the strategy may disappear and even has a negative effect on the thermal conductivity of composites. The variation tendencies of the thermal conductivities of composites in the present experiment reflect this behavior very well.

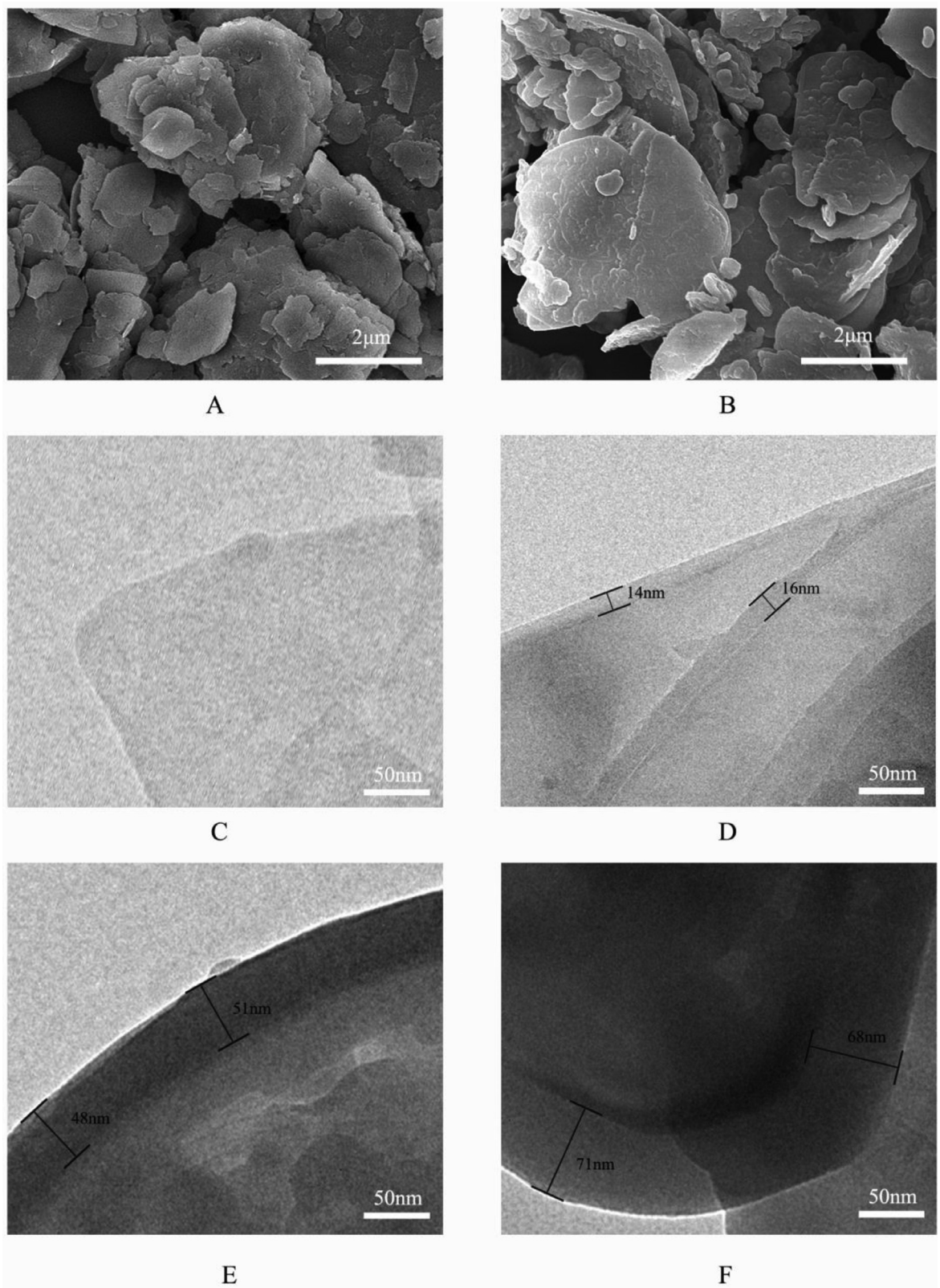

Fig. 4. SEM images of (A) pristine BN and (B) BN@SiO_2. TEM images of (C) pristine BN and BN@SiO_2 with (D) 15 nm, (E) 50 nm and (F) 70 nm silica coating thickness.

Interestingly, unlike the common understanding that increasing the filler content has a positive effect on the thermal conduction enhancement, even though coating a thin nanolayer on the filler surface, the effects of using the strategy will vary with the filler content. When the filler content increased from 20 vol.% to 30 vol.%, the thermal conductivity of epoxy/BN@SiO_2(15 nm) composites was lower than that of the epoxy/BN composites. In other words, the coating thickness is not the only factor that matters and filler content can significantly influence the results of nanolayer coating strategy. In order to investigate the effect of filler content

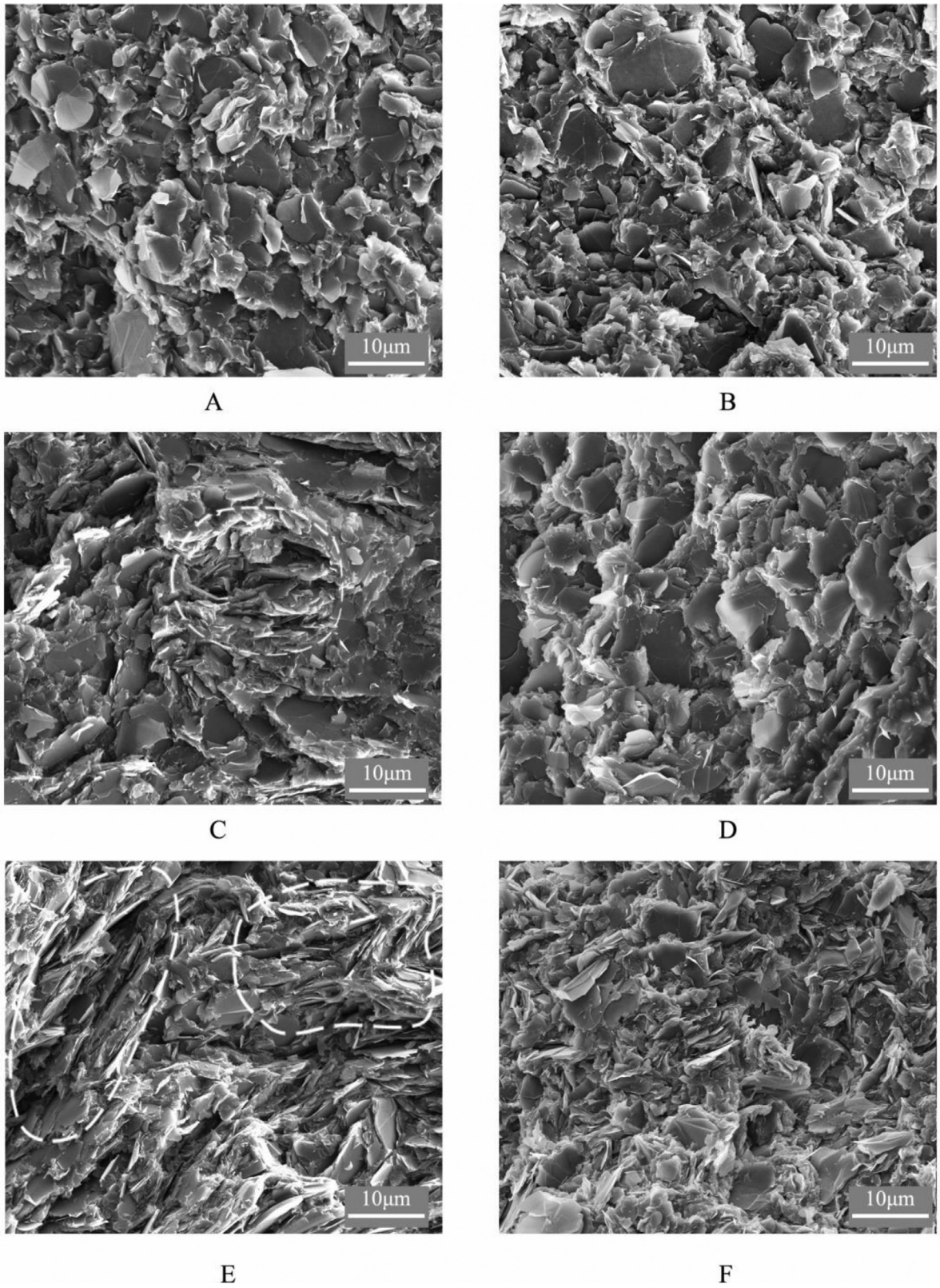

Fig. 5. SEM images of the fracture surfaces of the epoxy composites with (A) 10, (C) 20, (E) 30 vol.% of BN, and the epoxy composites with (B) 10, (D) 20, (F) 30 vol.% of BN@SiO_2, respectively.

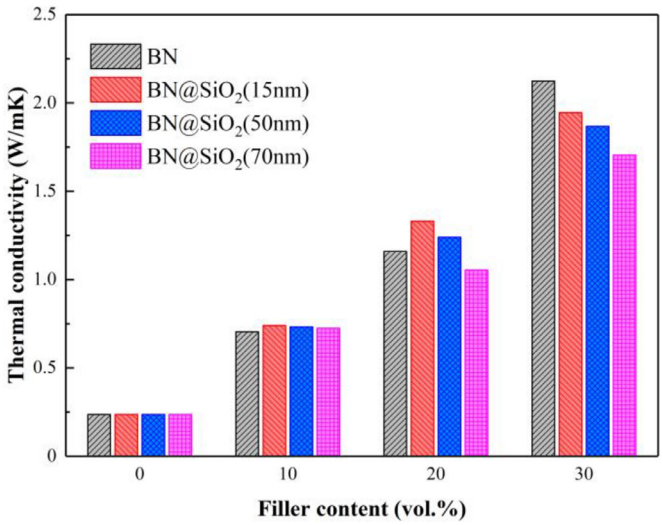

Fig. 6. Thermal conductivities of epoxy/BN composites and epoxy/BN@SiO_2 composites at different filler contents.

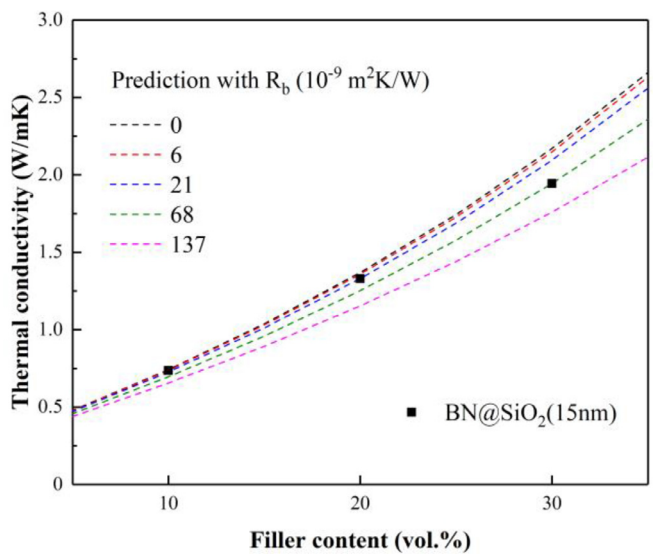

Fig. 7. The measured thermal conductivity (dots) of the epoxy/BN@SiO_2(15 nm) composites at different filler contents and the predicted thermal conductivity (dash lines) from EMA with consideration of R_b.

on thermal conduction enhancement in this strategy, a modified effective medium approximation (EMA) [38] which concerns the effects of particle geometry, orientation and interfacial thermal resistance is applied to analyze the experimental data (The details of EMA model are presented in supporting information). Considering the filler content has no influence on the particle geometry and the arbitrary orientation, by fitting the measured thermal conductivity to the EMA prediction, the interfacial thermal resistance (R_b) of the epoxy/BN@SiO_2(15 nm) composites at different filler content is extracted and analyzed [39–41]. The EMA prediction with consideration of R_b and the measured thermal conductivity are shown in Fig. 7. The fitted R_b of the epoxy/BN@SiO_2(15 nm) composites was 6×10^{-9} m^2K/W at 10 vol.%, 21×10^{-9} m^2K/W at 20 vol.% and 68×10^{-9} m^2K/W at 30 vol.%, respectively. It's interesting to note that the interfacial thermal resistance significantly increases with the increase of filler content. However, the interfacial interaction between the BN@SiO_2 and epoxy resin is mainly affected by

Table 1
Thermal conductive characteristic equation and coefficients of the Y.Agari model.

Filler	C_m	C_p	Y.Agari Model
Pristine BN	1.705	0.794	$k = 10^{(2.362f\ -\ 0.395)}$
BN@SiO_2(15 nm)	2.056	0.720	$k = 10^{(2.098f\ -\ 0.314)}$
BN@SiO_2(50 nm)	2.002	0.689	$k = 10^{(2.032f\ -\ 0.326)}$
BN@SiO_2(70 nm)	1.949	0.614	$k = 10^{(1.858f\ -\ 0.337)}$

the chemical and physical properties of BN@SiO_2 particles rather than the filler content. The changes in interfacial thermal resistance between the filler and polymer matrix should not be considered as a reasonable cause for the behavior. Through the fracture surface morphology of composites, the particle distribution could give important insights into the heat transfer in the composites. When the filler content is increased, the monodisperse particles gradually come into contact with each other to form a thermal conduction network. However, due to the low thermal conductivity of the nanolayer, the heat transfer in the thermal conduction network will be restrained. With the formation of thermal conduction network, the interfacial thermal resistance between the filler and filler is gradually increased in the strategy. Therefore, as the filler content increases, the increased total interfacial thermal resistance will deteriorate the enhanced effect of filler surface coating strategy on thermal conduction.

In order to systematically investigate the effects of both coating thickness and filler content on the thermal conduction enhancement, Y.Agari model which considered the formation of thermal conduction paths within the polymer matrix was selected to estimate the thermal conductivity of composites [42,43]. The logarithmic equation of Y.Agari model is given in Eq. (1):

$$\log k = fC_p \log k_p + (1 - f)\log(C_m k_m) \tag{1}$$

where C_m represents the effect of the fillers on the polymer crystallinity or crystal size and C_p represents the capability of the fillers to form a thermal conductive chain through the material. The thermal conductive characteristic equation and the calculated C_m and C_p values of the Y.Agari model are listed in Table 1. Due to the strong interfacial interaction between the BN@SiO_2 and epoxy matrix, the C_m of epoxy/BN@SiO_2 composites is higher than that of the epoxy/BN composites. However, the poor thermal conductivity of the silica nanolayer leads to bad heat transfer in the BN@SiO_2 thermal conductive network, the C_p of epoxy/BN@SiO_2 composites is lower than that of the epoxy/BN composites. The thermal conductivity curve of the composites estimated by the Y.Agari model is depicted in Fig. 8, and the predicted thermal conductivity of composites was fitted very well with the experimental value. And then the thermal conduction enhancement of the composites using the nanolayer coating strategy was evaluated by the enhancement factor (η) which can be calculated by the following equation:

$$\eta = \frac{k_n - k_c}{k_c} \times 100\% \tag{2}$$

where k_c is the thermal conductivity of composites incorporated with pristine filler, k_n is the thermal conductivity of composites incorporated with modified filler under the same filler content.

The contour plot of the enhancement factor is shown in Fig. 9. As the filler content increased, the developed thermal conduction networks within the polymer matrix were found to have a negative effect on the enhancement factor. And as depicted in Fig. 10, this behavior also can be observed in other material systems that use the nanolayer coating strategy to improve the thermal conductivity [15,27,44–46]. Thus, there is a concept of the effective filler volume fraction in the strategy, and within the effective filler volume fraction, the nanolayer coating strategy can truly enhance the ther-

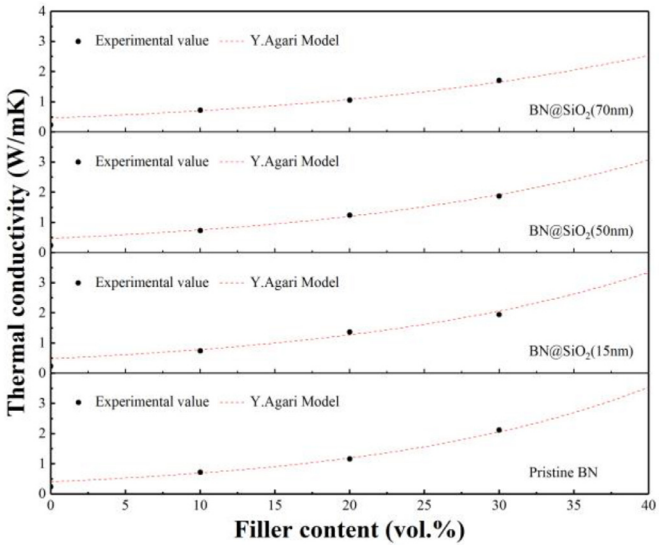

Fig. 8. The experimental value and Y.Agari model estimated value of the thermal conductivities of the epoxy/BN composites and epoxy/BN@SiO_2 composites at different filler contents.

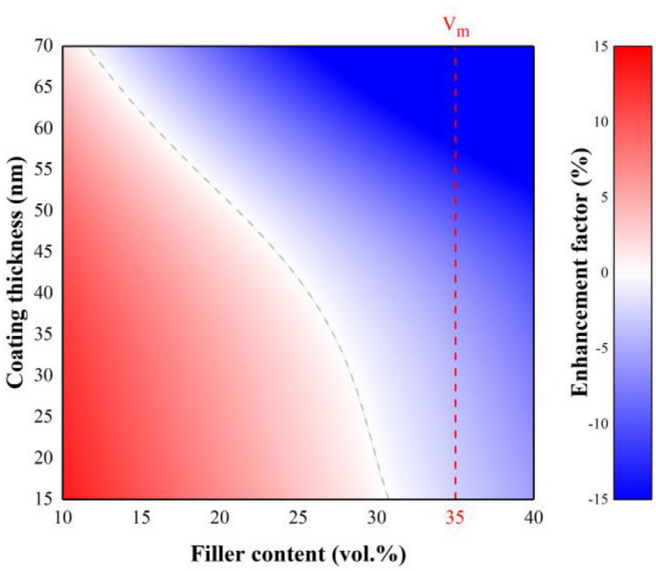

Fig. 9. The enhancement factor of the epoxy/BN@SiO_2 composites at different filler contents and coating thicknesses.

mal conduction in the composites. As the coating thickness gradually decreased, the volume fraction corresponding to zero enhancement factor was getting closer to 35 vol.%, which exactly has been proved as the maximum random packing volume fraction of the BN flaky particles used in the present work [47]. Even though reducing the coating thickness will expand the effective filler volume fraction, the upper limit of the effective filler volume fraction will not beyond the maximum random packing volume fraction of the fillers.

In order to make a better understanding of the thermal conductive effects and mechanism of the nanolayer coating strategy on the composites, a schematic diagram of thermal conduction in the composites is shown in Fig. 11. As shown in Fig. 11A, B, E and F, the silica nanolayer coated BN is dispersed more homogeneous than pristine BN in the epoxy matrix. Within the effective filler volume fraction, the modified filler surface chemical and physical properties significantly enhance the interfacial interaction between

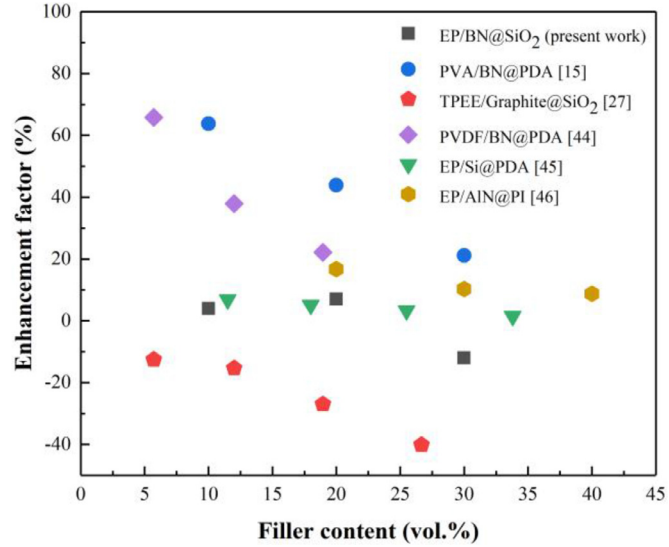

Fig. 10. The enhancement factor of other material systems which use the nanolayer coating strategy to improve the thermal conduction.

the filler and matrix and improve the dispersion of fillers, which provides more opportunity for the filler to form a local thermal conductive path to enhance the thermal conduction in the composites [17,48]. However, as depicted in Fig. 11C, D, G and H, with the filler content growing up, both the thermal conduction islands of pristine BN and the local thermal conduction paths of BN@SiO_2 can contact each other to build thermal conduction networks in the epoxy matrix, respectively. The formed thermal conduction networks will become the preferred heat flux path in the composites and main contributor to the thermal conduction enhancement. But the BN particles cannot directly contact each other in the BN@SiO_2 thermal conduction networks and the heat transfer is hindered in the silica coating layer, which leads to the greater interfacial thermal resistance among the BN@SiO_2 thermal conduction networks than that among the pristine BN thermal conduction networks. As a result, with increasing the filler content, the thermal conduction networks are developing, but the thermal conduction enhancement of the composites using nanolayer coating strategy is deteriorating. And before the thermal conduction networks are fully formed at the maximum random packing volume fraction of fillers, with decreasing the coating thickness, the effective filler volume fraction will get expanded because of the interfacial thermal resistance reduction in the modified filler thermal conduction networks.

In summary, as shown in Fig. 12, although coating the filler surface with a nanolayer will effectively improve the filler dispersion and enhance the interfacial interaction between the filler and matrix, the biggest drawback of the strategy is that the thermal conductivity of the nanolayer is generally lower than that of the fillers resulting in a large interfacial thermal resistance existed in the modified filler thermal conduction networks. Thus, in a definite nanolayer coating strategy, the coating thickness and filler content are the main two factors that determine the enhanced effect of the strategy on thermal conduction. Reducing the coating thickness will increase the enhanced effect of the strategy and expand the effective filler volume fraction. But influenced by the interfacial thermal resistance existed in the thermal conduction networks, the maximum effective filler volume fraction is no more than the maximum random packing volume fraction of the fillers.

4. Conclusion

In this work, the effects and mechanism of the filler surface coating strategy on the thermal conductivity of composites were

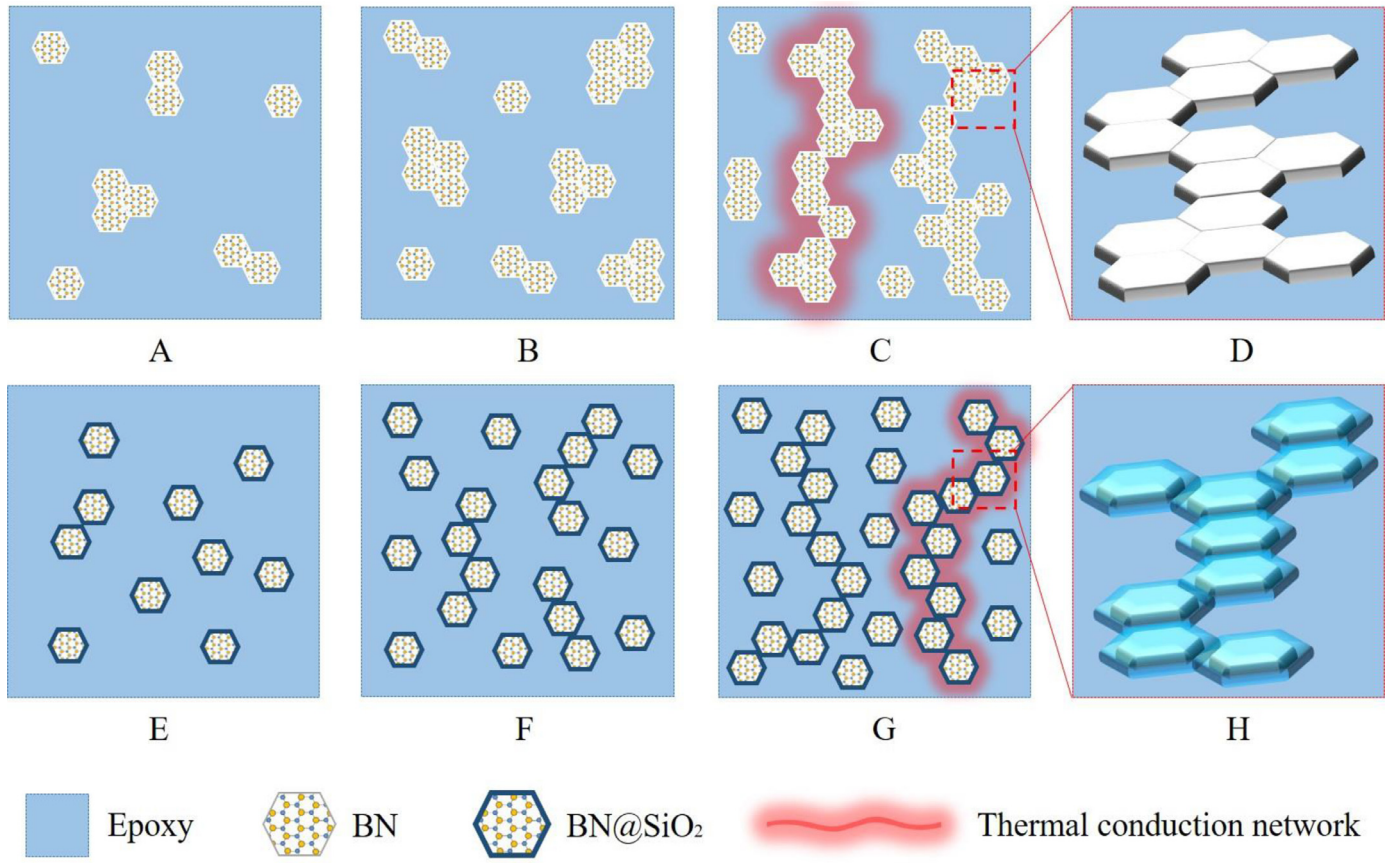

Fig. 11. The schematic diagrams of thermal conduction in the epoxy composites with (A) 10, (B) 20 and (C, D) 30 vol.% of BN, and in the epoxy composites with (E) 10, (F) 20 and (G, H) 30 vol.% of BN@SiO_2, respectively.

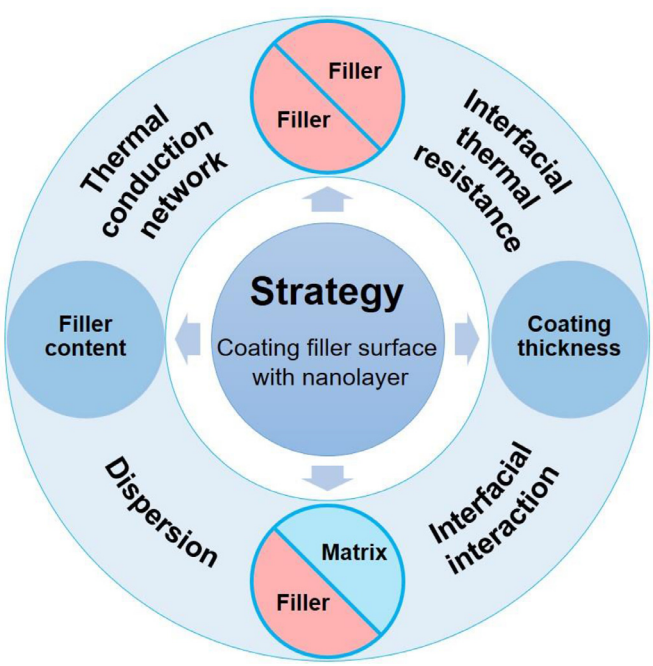

Fig. 12. The effects and mechanism of the nanolayer coating strategy on the thermal conductivity of composites.

systematically analyzed and clearly presented by investigating the thermal conductivity of epoxy/BN@SiO_2 composites. In a definite nanolayer coating strategy, the enhanced effect of the strategy on thermal conduction is significantly influenced by the coating thickness and filler content. And the concept of the effective filler volume fraction is introduced in the strategy for the first time. Within the effective filler volume fraction, the nanolayer coating strategy can truly enhance the thermal conduction in the composites. Although the filler dispersion and interfacial interaction between the filler and matrix are enhanced in the strategy, the heat transfer in the coating layer is hindered. Reducing the coating thickness will decrease the interfacial thermal resistance among the filler and between the filler and polymer matrix, which will increase the enhanced effect of the strategy and expand the effective filler volume fraction. And the interfacial thermal resistance of the composites filled with nanolayer coated filler was analyzed by the EMA approximation. As the filler content increased, the interfacial thermal resistance between the filler and filler is gradually increased with the formation of thermal conduction network, which has a negative effect on the thermal conduction enhancement of the strategy. And restrained by the interfacial thermal resistance existed in the thermal conduction networks, the upper limit of the effective filler volume fraction will not beyond the maximum random packing volume fraction of the fillers. We expect that the comprehensive understanding of this issue provided in the study will make a benefit for the design of thermal management materials.

Declaration of Competing Interest

None declared.

CRediT authorship contribution statement

Yunmin Liang: Conceptualization, Methodology, Validation, Formal analysis, Data curation, Writing - original draft, Writing -

review & editing. **Biwei Liu:** Investigation, Validation. **Bo Zhang:** Investigation. **Zhichun Liu:** Resources, Conceptualization, Supervision, Writing - review & editing, Project administration, Funding acquisition. **Wei Liu:** Resources, Supervision, Project administration.

Acknowledgements

The research was financially supported by the National Natural Science Foundation of China (No. 51776079).

Supplementary materials

Supplementary material associated with this article can be found, in the online version, at doi:10.1016/j.ijheatmasstransfer.2020.120533.

References

[1] J. Hansson, T.M.J. Nilsson, L. Ye, J. Liu, Novel nanostructured thermal interface materials: a review, Int. Mater. Rev. 63 (1) (2017) 22–45.
[2] A.L. Moore, L. Shi, Emerging challenges and materials for thermal management of electronics, Mater. Today 17 (4) (2014) 163–174.
[3] K.M. Razeeb, E. Dalton, G.L.W. Cross, A.J. Robinson, Present and future thermal interface materials for electronic devices, Int. Mater. Rev. 63 (1) (2017) 1–21.
[4] H. Chen, V.V. Ginzburg, J. Yang, Y. Yang, W. Liu, Y. Huang, L. Du, B. Chen, Thermal conductivity of polymer-based composites: fundamentals and applications, Prog. Polym. Sci. 59 (2016) 41–85.
[5] N. Burger, A. Laachachi, M. Ferriol, M. Lutz, V. Toniazzo, D. Ruch, Review of thermal conductivity in composites: mechanisms, parameters and theory, Prog. Polym. Sci. 61 (2016) 1–28.
[6] X. Xu, J. Chen, J. Zhou, B. Li, Thermal conductivity of polymers and their nanocomposites, Adv. Mater. 30 (17) (2018) 1705544.
[7] Y.-.X. Fu, Z.-.X. He, D.-C. Mo, S.-S. Lu, Thermal conductivity enhancement with different fillers for epoxy resin adhesives, Appl. Therm. Eng. 66 (1–2) (2014) 493–498.
[8] J. Gu, Y. Guo, X. Yang, C. Liang, W. Geng, L. Tang, N. Li, Q. Zhang, Synergistic improvement of thermal conductivities of polyphenylene sulfide composites filled with boron nitride hybrid fillers, Composites, Part A 95 (2017) 267–273.
[9] S. Wang, Y. Cheng, R. Wang, J. Sun, L. Gao, Highly thermal conductive copper nanowire composites with ultralow loading: toward applications as thermal interface materials, ACS Appl. Mater. Interfaces 6 (9) (2014) 6481–6486.
[10] M.W. Akhtar, Y.S. Lee, D.J. Yoo, J.S. Kim, Alumina-graphene hybrid filled epoxy composite: quantitative validation and enhanced thermal conductivity, Compos. Part B 131 (2017) 184–195.
[11] J. Gu, X. Yang, Z. Lv, N. Li, C. Liang, Q. Zhang, Functionalized graphite nanoplatelets/epoxy resin nanocomposites with high thermal conductivity, Int. J. Heat Mass Transf. 92 (2016) 15–22.
[12] J. Gu, C. Liang, X. Zhao, B. Gan, H. Qiu, Y. Guo, X. Yang, Q. Zhang, D.-.Y. Wang, Highly thermally conductive flame-retardant epoxy nanocomposites with reduced ignitability and excellent electrical conductivities, Compos. Sci. Technol. 139 (2017) 83–89.
[13] Y. Jiang, X. Shi, Y. Feng, S. Li, X. Zhou, X. Xie, Enhanced thermal conductivity and ideal dielectric properties of epoxy composites containing polymer modified hexagonal boron nitride, Compos., Part A 107 (2018) 657–664.
[14] C. Pan, K. Kou, Q. Jia, Y. Zhang, G. Wu, T. Ji, Improved thermal conductivity and dielectric properties of hBN/PTFE composites via surface treatment by silane coupling agent, Compos. Part B 111 (2017) 83–90.
[15] H. Shen, J. Guo, H. Wang, N. Zhao, J. Xu, Bioinspired modification of h-BN for high thermal conductive composite films with aligned structure, ACS Appl. Mater. Interfaces 7 (10) (2015) 5701–5708.
[16] A. Xie, Y. Wang, P. Jiang, S. Li, X. Huang, Nondestructive functionalization of carbon nanotubes by combining mussel-inspired chemistry and RAFT polymerization: towards high dielectric nanocomposites with improved thermal management capability, Compos. Sci. Technol. 154 (2018) 154–164.
[17] C. Chen, Y. Tang, Y.S. Ye, Z. Xue, Y. Xue, X. Xie, Y.-.W. Mai, High-performance epoxy/silica coated silver nanowire composites as underfill material for electronic packaging, Compos. Sci. Technol. 105 (2014) 80–85.
[18] Y. Wang, X. Qiu, J. Zheng, Study the mechanism that carbon nanotubes improve thermal stability of polymer composites: an ingenious design idea with coating silica on CNTs and valuable in engineering applications, Compos. Sci. Technol. 167 (2018) 529–538.
[19] K. Ahn, K. Kim, J. Kim, Fabrication of surface-treated BN/ETDS composites for enhanced thermal and mechanical properties, Ceram. Int. 41 (8) (2015) 9488–9495.
[20] M.K. Hassanzadeh-Aghdam, M.J. Mahmoodi, J. Jamali, Effect of CNT coating on the overall thermal conductivity of unidirectional polymer hybrid nanocomposites, Int. J. Heat Mass Transf. 124 (2018) 190–200.
[21] S.I. Kundalwal, R. Suresh Kumar, M.C. Ray, Effective thermal conductivities of a novel fuzzy fiber-reinforced composite containing wavy carbon nanotubes, J. Heat Transf. 137 (1) (2015).
[22] W. Stöber, A. Fink, E. Bohn, Controlled growth of monodisperse silica spheres in the micron size range, J. Colloid Interface Sci. 26 (1) (1968) 62–69.
[23] W. Yan, Y. Zhang, H. Sun, S. Liu, Z. Chi, X. Chen, J. Xu, Polyimide nanocomposites with boron nitride-coated multi-walled carbon nanotubes for enhanced thermal conductivity and electrical insulation, J. Mater. Chem. A 2 (48) (2014) 20958–20965.
[24] H. Lee, S.M. Dellatore, W.M. Miller, P.B. Messersmith, Mussel-inspired surface chemistry for multifunctional coatings, Science 318 (5849) (2007) 426.
[25] Y. Jiang, M. Li, C. Chen, Z. Xue, X. Xie, X. Zhou, Y.-W. Mai, Effect of elastic modulus mismatch of epoxy/titanium dioxide coated silver nanowire composites on the performance of thermal conductivity, Compos. Sci. Technol. 165 (2018) 206–213.
[26] R. Sun, H. Yao, H.-.B. Zhang, Y. Li, Y.-.W. Mai, Z.-.Z. Yu, Decoration of defect-free graphene nanoplatelets with alumina for thermally conductive and electrically insulating epoxy composites, Compos. Sci. Technol. 137 (2016) 16–23.
[27] S. Choi, K. Kim, J. Nam, S.E. Shim, Synthesis of silica-coated graphite by enolization of polyvinylpyrrolidone and its thermal and electrical conductivity in polymer composites, Carbon N Y 60 (2013) 254–265.
[28] K. Kim, K. Ahn, H. Ju, J. Kim, Improvement of insulating and thermal properties of SiO2-coated copper nanowire composites, Ind. Eng. Chem. Res. 55 (10) (2016) 2713–2720.
[29] H. Yuan, Y. Wang, T. Li, P. Ma, S. Zhang, M. Du, M. Chen, W. Dong, W. Ming, Highly thermal conductive and electrically insulating polymer composites based on polydopamine-coated copper nanowire, Compos. Sci. Technol. 164 (2018) 153–159.
[30] H. Chen, C. Xu, G. Xiao, Z. Chen, J. Ma, G. Wu, Synthesis of (h-BN)/SiO2 core–shell powder for improved self-lubricating ceramic composites, Ceram. Int. 42 (4) (2016) 5504–5511.
[31] R. Al-Oweini, H. El-Rassy, Synthesis and characterization by FTIR spectroscopy of silica aerogels prepared using several Si(OR)4 and R′′Si(OR′)3 precursors, J. Mol. Struct. 919 (1–3) (2009) 140–145.
[32] K.S. Park, D.Y. Lee, K.J. Kim, D.W. Moon, Observation of a hexagonal BN surface layer on the cubic BN film grown by dual ion beam sputter deposition, Appl. Phys. Lett. 70 (3) (1997) 315–317.
[33] W. Cai, W. Guo, Y. Pan, J. Wang, X. Mu, X. Feng, B. Yuan, B. Wang, Y. Hu, Polydopamine-bridged synthesis of ternary h-BN@PDA@SnO 2 as nanoenhancers for flame retardant and smoke suppression of epoxy composites, Compos., Part A 111 (2018) 94–105.
[34] X. Zhang, Y. Wu, S. He, D. Yang, Structural characterization of sol–gel composites using TEOS/MEMO as precursors, Surf. Coat. Technol. 201 (12) (2007) 6051–6058.
[35] D. Yang, Y. Ni, X. Kong, D. Gao, Y. Wang, T. Hu, L. Zhang, Mussel-inspired modification of boron nitride for natural rubber composites with high thermal conductivity and low dielectric constant, Compos. Sci. Technol. 177 (2019) 18–25.
[36] G. Ragosta, M. Abbate, P. Musto, G. Scarinzi, L. Mascia, Epoxy-silica particulate nanocomposites: chemical interactions, reinforcement and fracture toughness, Polymer (Guildf) 46 (23) (2005) 10506–10516.
[37] R. Pal, Thermal conductivity of three-component composites of core-shell particles, Mater. Sci. Eng. 498 (1–2) (2008) 135–141.
[38] C.-.W. Nan, R. Birringer, D.R. Clarke, H. Gleiter, Effective thermal conductivity of particulate composites with interfacial thermal resistance, J. Appl. Phys. 81 (10) (1997) 6692–6699.
[39] Z. Lin, Y. Liu, S. Raghavan, K.S. Moon, S.K. Sitaraman, C.P. Wong, Magnetic alignment of hexagonal boron nitride platelets in polymer matrix: toward high performance anisotropic polymer composites for electronic encapsulation, ACS Appl. Mater. Interfaces 5 (15) (2013) 7633–7640.
[40] C. Yuan, B. Duan, L. Li, B. Xie, M. Huang, X. Luo, Thermal conductivity of polymer-based composites with magnetic aligned hexagonal boron nitride platelets, ACS Appl. Mater. Interfaces 7 (23) (2015) 13000–13006.
[41] C. Yuan, B. Xie, M. Huang, R. Wu, X. Luo, Thermal conductivity enhancement of platelets aligned composites with volume fraction from 10% to 20%, Int. J. Heat Mass Transf. 94 (2016) 20–28.
[42] Y. Agari, T. Uno, Estimation on thermal conductivities of filled polymers, J. Appl. Polym. Sci. 32 (7) (1986) 5705–5712.
[43] Y. Agari, A. Ueda, M. Tanaka, S. Nagai, Thermal conductivity of a polymer filled with particles in the wide range from low to super-high volume content, J. Appl. Polym. Sci. 40 (5-6) (1990) 929–941.
[44] D.-.L. Zhang, J.-W. Zha, W.-K. Li, C.-Q. Li, S.-J. Wang, Y. Wen, Z.-M. Dang, Enhanced thermal conductivity and mechanical property through boron nitride hot string in polyvinylidene fluoride fibers by electrospinning, Compos. Sci. Technol. 156 (2018) 1–7.
[45] Z. Wang, Y. Cheng, M. Yang, J. Huang, D. Cao, S. Chen, Q. Xie, W. Lou, H. Wu, Dielectric properties and thermal conductivity of epoxy composites using core/shell structured Si/SiO2/Polydopamine, Compos. Part B 140 (2018) 83–90.
[46] Y. Zhou, Y. Yao, C.Y. Chen, K. Moon, H. Wang, C.P. Wong, The use of polyimide–modified aluminum nitride fillers in AlN@PI/epoxy composites with enhanced thermal conductivity for electronic encapsulation, Sci. Rep. 4 (2014) 4779.
[47] A. Wouterse, S.R. Williams, A.P. Philipse, Effect of particle shape on the density and microstructure of random packings, J. Phys. Condens. Matter 19 (40) (2007) 406215.
[48] S. Shenogin, A. Bodapati, L. Xue, R. Ozisik, P. Keblinski, Effect of chemical functionalization on thermal transport of carbon nanotube composites, Appl. Phys. Lett. 85 (12) (2004) 2229–2231.